Original Article

Cell Transplantation
1–12

DOI: 10.1177/0963689719842161
journals.sagepub.com/home/cll
SAGE

Bexarotene Exerts Protective Effects Through Modulation of the Cerebral Vascular Smooth Muscle Cell Phenotypic Transformation by Regulating PPARγ/FLAP/LTB_4 After Subarachnoid Hemorrhage in Rats

Zhaosi Zhang[1], Guosheng Zhao[2], Liu Liu[1], Junchi He[1], Rami Darwazeh[1], Han Liu[1], Hong Chen[1], Chao Zhou[1], Zongduo Guo[1], and Xiaochuan Sun[1]

Abstract

Vascular smooth muscle cells (VSMCs) play an important role after a subarachnoid hemorrhage (SAH). The changes in VSMCs following bexarotene treatment after SAH are unknown. In the present study, neurological impairment, decreased cerebral cortical blood flow and transformation of cerebral VSMCs from a contractile to a synthetic phenotype were observed after SAH. Bexarotene reduced neurological impairment, improved cerebral cortical blood flow, inhibited VSMC phenotypic transformation and suppressed the expression of 5-lipoxygenase-activating protein (FLAP) and leukotriene B4 (LTB_4), which was partly reversed by GW9662, an inhibitor of peroxisome proliferator-activated receptor gamma (PPARγ). Mechanistically, sh-PPARγ-mediated phenotypic transformation of VSMCs was partially suppressed by MK886, an antagonist of FLAP. Therefore, we conclude that bexarotene reduced neurological impairment, improved cerebral cortical blood flow and inhibited the VSMC phenotypic transformation after SAH, which was achieved by activating PPARγ-mediated inhibition of FLAP/LTB_4 in VSMCs

Keywords

Bexarotene, subarachnoid hemorrhage, vascular smooth muscle cells, PPARγ, FLAP

Introduction

Subarachnoid hemorrhage (SAH) is frequently a devastating disease. SAH causes a greater than 50% combined morbidity and mortality rate. At present, diagnosis and surgical treatment of SAH has been improving. However, effective therapeutic interventions are still limited, and clinical outcomes remain disappointing[1]. Thus, novel effective therapies for SAH are urgently required. Recently, Zhang et al. proposed the concept of the vascular neural network, in which astrocytes, microglia, endothelial vascular smooth muscle cells (VSMCs) and pericytes participate in cerebrovascular physiology and pathology. VSMCs play an important role in neurovascular injury after SAH[2]. In addition, animal studies revealed that VSMCs transformed from a contractile to a synthetic phenotype after SAH. Interfering with this phenotypic transformation improves neurological function after SAH[3,4]. We therefore sought to further study the pathological and physiological process of VSMC phenotypic transformation after SAH.

Leukotriene B4 (LTB_4) plays an important role in the phenotypic transformation of VSMCs. LTB_4 promotes

[1] Department of Neurosurgery, The First Affiliated Hospital of Chongqing Medical University, Chongqing, China
[2] Department of Orthopedic Surgery, The First Affiliated Hospital of Chongqing Medical University, Chongqing, China

Submitted: September 8, 2018. Revised: November 30, 2018. Accepted: December 13, 2018.

Corresponding Author:
Zongduo Guo, Department of Neurosurgery, The First Affiliated Hospital of Chongqing Medical University, Chongqing 400016, China.
Email: stonegzd@163.com

inflammatory cell chemotaxis, increases proinflammatory cytokine levels, deteriorates vascular permeability, modulates VSMC phenotypic transformation, and initiates VSMC migration and proliferation, resulting in blood vessel abnormalities[5–7]. Mechanistically, the 5-lipoxygenase-activating protein (FLAP) binds to 5-lipoxygenase(5-LOX) and arachidonic acid (AA) during leukotriene biosynthesis, facilitating AA translocation from the extracellular matrix to the nuclear membrane and promoting LTB_4 synthesis[8,9]. Studies have shown that abnormal FLAP expression in myeloid cells promoted LTB_4-dependent VSMC phenotypic transformation, intimal migration, and proliferation[10]. Despite these findings, the underlying mechanism regulating VSMC phenotypic transformation in SAH is poorly understood.

Recent studies have observed a correlation between LTB_4 and peroxisome proliferator-activated receptor gamma (PPARγ). Sobrado et al. reported that PPARγ activation by rosiglitazone inhibited LTB_4 expression in a middle-cerebral-artery-occlusion model[11]. Adrian et al. found that PPARγ and LTB_4 interact in the pathogenesis of pancreatic cancer[12]. Additionally, PPARγ was found to regulate the activation of 5-LOX, participating in tissue repair and anti-inflammatory processes after stroke[13]. PPARγ, a ligand-activated transcription factor that influences the expression of a number of genes, is currently thought to play an important role in the resolution of inflammation. Moreover, PPARγ has been found to play an important role in reducing inflammation and brain injury after SAH[14,15]. Moreover, studies have shown that PPARγ can inhibit VSMC phenotypic transformation[16,17,18]. However, the connection between PPARγ and LTB_4 in VSMCs after SAH is unclear.

Bexarotene is used clinically to treat refractory cutaneous T-cell lymphoma[19,20]. Some studies have reported that bexarotene exhibited a protective effect in some diseases of the central nervous system (CNS) such as amyotrophic lateral sclerosis[21], epilepsy[22], and Parkinson's disease[23]. In addition, bexarotene can activate PPARγ and binds to specific DNA sequences called peroxisome proliferator response elements (PPREs) in target gene promoters. Bexarotene has been shown to activate PPARγ to reduce inflammation and tissue injury during endotoxemia in rats[24]. Moreover, PPARγ activation regulates PPREs and other signaling pathways that inhibit inflammation and promote protection and repair in the brain[25,26]. However, few studies have explored the role bexarotene plays in SAH.

Therefore, the present study investigated the potentially protective role of bexarotene after SAH with respect to the phenotypic transformation of VSMCs mediated by PPARγ and FLAP/LTB_4 in cerebral vessels.

Materials and Methods

SAH Model and Experimental Protocol

All animal procedures were approved by the Ethics Committee of the First Affiliated Hospital of Chongqing Medical University, China. Briefly, adult male Sprague–Dawley (SD) rats weighing 300–400 g were chosen for the experiments. Anesthesia was induced by administering 3% isoflurane with 67% N_2O and 30% O_2 until rats became unresponsive to the tail pinch test; pentobarbital (50 mg/kg) was then injected peritoneally to maintain anesthesia. Each group included 12 rats, with a total of 204 rats used. The rats were randomly divided into the following groups in part 1: (1) Sham, (2) SAH 1d, (3) SAH 2d, (4) SAH 3d, (5) SAH 4d, (6) SAH 5d, and (7) SAH 7d. In the subsequent experiments, rats were tested for neurological function three days after SAH and then euthanized to determine the brain water content and SAH grading, as well as to perform immunofluorescence, western blotting, and enzyme-linked immunosorbent assay (ELISA). The experimental groups were as follows for part 2: (1) Sham, (2) SAH+vehicle, (3) SAH+bexarotene, and (4) SAH+bexarotene+GW9662. Rats were further divided into the following groups for part 3: (1) Sham, (2) SAH+sh-control, (3) SAH+sh-PPARγ1, (4) SAH+sh-PPARγ2, (5) SAH+MK886, and (6) SAH+sh-PPARγ+MK886.

A 3-0 sharpened monofilament nylon suture was gently inserted rostrally into the right internal carotid artery from the external carotid artery until the stump reached the bifurcation of the anterior and middle cerebral arteries. The suture was then advanced an additional 5 mm to perforate the artery, then immediately withdrawn, and the external carotid artery was ligated. Sham-operated rats were subjected to all surgical procedures except the suture puncture[27].

Drug Preparation and Administration

Drug preparation and administration were previously described by Zhong et al.[28] Briefly, 20 mg bexarotene (Selleck, Shanghai, China) was dissolved in 5.7 ml dimethyl sulfoxide (DMSO), and 51.3 ml phosphate-buffered saline (PBS) was added to the mixture. Similarly, 10 mg GW9662 (Selleck), an inhibitor of PPARγ was dissolved in 3.6 ml DMSO, and PBS (32.4 ml) was added to the mixture. A total of 10 mg of MK886 (Selleck), an antagonist of FLAP was dissolved in 2.1 ml DMSO, and 18.9 ml PBS was added to the mixture. The final concentrations of GW9662, MK886 and bexarotene were the same (1 mM). The solution was injected intraperitoneally at 5 mg/kg bexarotene, 2 mg/kg GW9662, and 3 mg/kg MK886 per day after SAH. The vehicle group solution was prepared in the same manner and administered in the same volume, same route and same time course as above. These reagents were used immediately after SAH and continued to be used once a day until the rats were euthanized.

Adenoviral Vectors of Short Hairpin RNAs

Adenoviral vectors expressing scrambled (control) or PPARγ short hairpin RNA (shRNA) (sh-PPARγ1 and sh-PPARγ2) to silence PPARγ transcription were

constructed by Hanbio (Shanghai, China). The resultant recombinant vector, pAd-sh-PPARγ, was digested with Pac I and transfected into AD-293 cells to package viral particles expressing sh-PPARγ (Ad-sh-PPARγ). The adenovirus was purified using a gradient-density ultracentrifugation of cesium chloride and dialyzed in dialysis buffer.

Viral vectors were injected into the lateral cerebral ventricle at a rate of 2 μl/min with 10 μl of 2 μM siRNA per the manufacturer's instructions. The vectors were stored at −80°C until used and then diluted to 1×10^{10} pfu/ml. A total of 10 μl of the dilution was injected into each animal. Rats were placed in a stereotaxic apparatus under pentobarbital (50 mg/kg) anesthesia, and their rectal temperature was maintained at 37.5°C using a feedback-controlled heating pad. A cranial burr hole (1 mm) was drilled into the skull 1.5 mm posterior and 1.0 mm lateral relative to the bregma. A needle was inserted through the burr hole 3.5 mm below the horizontal plane of the bregma into the right lateral ventricle 3 days before SAH to obtain maximum amplification.

Neurological Scoring

At 3 days after SAH, an observer blinded to the experimental groups used a modified Garcia score system to assess sensorimotor functions. The evaluation consisted of six tests with scores ranging from 3 to 18: spontaneous activity (0–3), symmetrical movements of four limbs (0–3), outstretching of forelimbs (0–3), climbing (1–3), body proprioception (1–3), and response to vibrissal touch (1–3). Lower scores indicated worse neurological function in the rats. The data from the pre-stroke tests were defined as the baseline[29].

Grading SAH Severity

The SAH grading system was used to blindly evaluate SAH severity immediately after euthanasia. Briefly, the brain was removed from the skull, and a photograph of the base of the brain was divided into six scored sections (0–3) based on the amount of subarachnoid blood. Each segment had a grade from 0 to 3 depending on the amount of subarachnoid blood clotting in the segment as follows: Grade 0: no subarachnoid blood; Grade 1: minimal subarachnoid blood; Grade 2: moderate blood clotting with recognizable arteries; and Grade 3: blood clotting obliterating all arteries within the segment. Under normal conditions, the score was 0 points. The total score was calculated as the sum of all section scores. Operated animals received a total score ranging from 0 (no SAH) to 18 (most severe SAH), and SAH rats with scores of 7 or less were excluded from the study[30].

Brain Water Content

Brain water content was detected using the wet/dry method[29]. Briefly, the cerebral hemispheres were removed from the skull, separately placed into pre-weighed and labelled glass vials, and weighed to obtain the wet weight. The vials were subsequently placed in an oven at 105°C for 24 h, and then they were reweighed to obtain the dry weight. The percentage of brain water content was calculated as [(wet weight – dry weight)/wet weight] × 100%.

Cerebral Cortical Blood Flow

Cerebral blood flow was determined using laser speckle flowmetry (GENE&I, Beijing, China) which obtains high-resolution two-dimensional (2D) images in seconds. Briefly, rats were anesthetized with pentobarbital (50 mg/kg), and their skulls were exposed and covered with plastic wrap. A 635-nm semiconductor laser illuminated the region of interest. The lens focus was adjusted until the region of interest filled the camera's field of view, which was connected by a fiberoptic cable to a laser speckle perfusion imaging (LSPI) instrument head that also contained a black and white charge-coupled device camera with a close-focus imaging zoom lens. Cerebral blood flow was measured in the region of the middle cerebral artery. The exposure time was set at 60 s. The LSPI camera output was fed directly to a live monitor to continuously record the laser-illuminated tissue. The intensity was accumulated in a charge-coupled device camera and transferred to a computer for analysis. High-resolution digital images were processed using custom LSPI algorithms to produce quantitative color-coded perfusion maps of tissue blood flow[31].

ELISA

Cerebral vascular tissues around the circle of Willis were mechanically homogenized in radioimmunoprecipitation assay (RIPA) lysis buffer (CW2333, CWBIO, Beijing, China). Lysates were centrifuged at 12,000 rpm for 20 minutes at 4°C, and the level of LTB_4 in the tissue was measured using ELISA (MBS762528, MyBioSource, CA, USA). The concentration of LTB_4 in the tissue was determined per the manufacturer's directions.

Western Blotting

Cerebral vascular tissues around the circle of Willis were mechanically homogenized in RIPA lysis buffer. A protease inhibitor cocktail (CW2200, CWBIO, Beijing, China) was added to inhibit protein degradation. An ultrasonic cell crusher was used to crack the tissues, and Eppendorf centrifuge was used to centrifuge the lysates at 15,300×*g* (12,000 rpm) for 20 min at 4°C. Protein concentrations were measured using the BCA Protein Assay Kit (Beyotime, Shanghai, China). Samples (50 μg per lane) were separated via 8% or 12% sodium dodecyl sulfate polyacrylamide gel electrophoresis (SDS-PAGE) and electrotransferred to a polyvinylidene difluoride membrane (Millipore, CA, USA). The membrane was blocked using 5% bovine serum albumin for 1 hour at 37°C and incubated overnight at 4°C with primary antibodies. The following antibodies were used: PPARγ

(A11183, ABclonal, Wuhan, China), α-smooth muscle actin (α-SMA; ab7817, Abcam, CA, USA), embryonic smooth muscle myosin heavy chain (Smemb; 19673-1-AP, Proteintech, Wuhan, China) and FLAP (OM205402, OmnimAbs, CA, USA). Glyceraldehyde-3-phosphate dehydrogenase (AB-P-R001, GAPDH; Goodhere Biotechnology, Hangzhou, China) was used as an internal reference. The membrane was washed three times for 5 min in tris-buffered saline (TBS)+Tween 20 and incubated with the appropriate horseradish peroxidase-conjugated secondary antibody (A0208, Beyotime, Shanghai, China) for 1 hour at 37°C. Densitometry analysis was performed using the ChemiDoc detection system and Quantity One software (Bio-Rad, CA, USA).

Immunofluorescence

Immunofluorescence was performed as described[3]. Briefly, immunofluorescence staining of brain tissues around the circle of Willis was performed on fixed frozen sections to analyze the morphometry of the middle cerebral artery (MCA). A total of 94 rats were anaesthetized 3 days after SAH using pentobarbital (50 mg/kg) and perfused transcardially with 4% paraformaldehyde (PFA). The cerebrum was removed and post-fixed in 4% PFA overnight at 4°C. The tissues were dehydrated with 20% sucrose overnight at 4°C, followed by 30% sucrose overnight at 4°C and embedded in optimal cutting temperature compound. The tissue was sectioned (10 μm thickness) using a cryostat (Leica, Germany) on glass coverslips for immunostaining. Microwave ovens were used for antigen retrieval in a citrate solution for 20 min. Endogenous peroxidase activity was blocked using 3% hydrogen peroxide for 15 min and rinsed in PBS. Transverse sections were incubated in a blocking solution (5% donkey serum, Solarbio Science and Technology Co., Ltd., Beijing, China) for 1 h at room temperature (RT). Sections were incubated with primary antibodies overnight at 4°C and secondary antibodies (1:200, Proteintech, Wuhan, China) for 1 h at RT. Cell nuclei were stained with 4',6-diamidino-2-phenylindole (DAPI; Sigma-Aldrich, CA, USA).

Fluorescence images were captured using a fluorescence microscope system (Leica, Germany). The diameter and wall thickness of the MCA were measured as described previously. Briefly, three sequential sections (the midpoint of the proximal, middle and distal) were taken for each vessel, measured, and averaged. The MCA diameter and wall thickness were measured using ImageJ software per the manufacturer's instructions. Briefly, the inner perimeter of the vessels was measured by tracing the entire luminal surface of the intima, and the diameter (d) of the vessels was calculated per the equivalent perimeter circle (d = measured inner perimeter/π). The vessel wall thickness was measured as the distance from the luminal surface of the intima to the outer border of the media at three points for each artery, and the three measurements were averaged for one score[3].

Statistical Analysis

GraphPad Prism 7.0 software was used for statistical analyses. A Chi-square test was used to compare mortality rates between groups. Behavior scores were found not normally distributed by a Shapiro–Wilk test. Therefore, the scores were compared using a Kruskal–Wallis test with Dunn's multiple comparison for post hoc, and the data were presented as a median with interquartile range. Other measurements were normally distributed through the Shapiro–Wilk test and were analyzed using either one-way or two-way analysis of variance (ANOVA) and presented as the mean with standard deviation. Further comparisons of the measurements between groups were performed using Dunnett's test. Statistical significance was set at $P<0.05$.

Results

Cerebral VSMCs Transformed from a Contractile Phenotype to a Synthetic Phenotype After SAH

Western blotting followed by ANOVA plus post hoc testing revealed that α-SMA expression was decreased and Smemb expression was increased in VSMCs, suggesting that VSMCs changed from contractile to synthetic after SAH (Fig 1A). The phenotypic transformation of VSMCs were obvious 3 days after SAH. Moreover, PPARγ and FLAP expression also reached relatively high levels (Fig 1A). Therefore, we chose the third day as the time point for observation and intervention in the subsequent experiments. Immunofluorescence (Fig 1B and C) revealed that PPARγ and FLAP were upgraded in VSMCs after SAH.

Bexarotene Reduced Neurological Impairment and Relieved the Decreased Cerebral Cortical Blood Flow via PPARγ Activation After SAH

We divided adult male rats into four groups to examine the protective role of bexarotene after subarachnoid hemorrhaging as follows: Sham, SAH+vehicle, SAH+bexarotene, and SAH+bexarotene+GW9662 (12 rats per group). We used modified Garcia scores (Fig 2A) to assess the neurological function of SD rats in the four groups 3 days after SAH. Mortality was assessed after SAH (Fig 2B). We used laser speckle to measure cerebral cortical blood flow in SD rats in the four groups (Fig 2C). The subarachnoid hemorrhage severity was determined using the SAH severity scores (Fig 2D). Brain water content was measured in the four groups (Fig 2E).

In general, bexarotene improved neurological function, reduced mortality, decreased SAH severity and reduced brain edema after SAH. Bexarotene relieved the decreased cerebral cortical blood flow after SAH. The specific antagonist of PPARγ, GW9662, partially counteracted these effects.

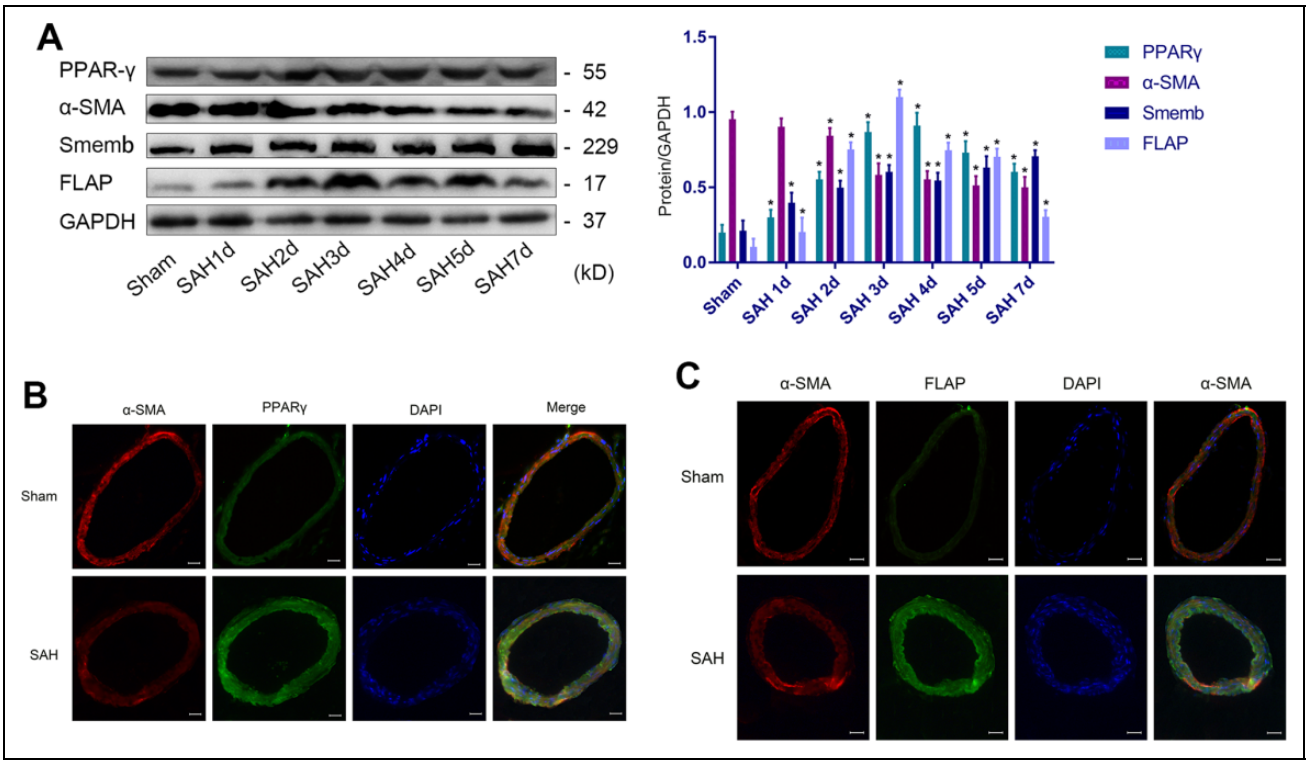

Figure 1. VSMC phenotypic transformation from 1 to 7 days after SAH. (A) Representative immunoblots and representative quantitative analyses of PPARγ, α-SMA, Smemb and FLAP (*P<0.05 versus Sham group). (B) Representative image and IF of PPARγ (green), α-SMA (red), and DAPI (blue) in cerebral vascular tissues (scale bar, 20 μm). (C) Representative image and immunofluorescence of FLAP (green), α-SMA (red), and DAPI (blue) in cerebral vascular tissues (scale bar, 20 μm; n=12, with 6 used for western blotting and 6 used for IF).
α-SMA: α-smooth muscle actin; DAPI: 4′,6-diamidino-2-phenylindole; FLAP: 5-lipoxygenase-activating protein; IF, immunofluorescence; PPARγ: peroxisome proliferator-activated receptor gamma; SAH: subarachnoid hemorrhage; Smemb: embryonic smooth muscle myosin heavy chain; VSMC: vascular smooth muscle cell.

Bexarotene Inhibited VSMC Phenotypic Transformation by Activating PPARγ After SAH

SD rats were divided into four groups to further explore the protective mechanism of bexarotene after SAH. We performed western blot assays and found bexarotene increased the protein level of the contractile phenotypic marker α-SMA and decreased the synthetic phenotypic marker Smemb in VSMCs after SAH (Fig 3A). In addition, bexarotene increased the expression of PPARγ and inhibited the expression of FLAP and LTB_4 (Fig 3A and B). Moreover, we performed an immunofluorescence assay and discovered bexarotene reduced VSMC phenotypic transformation from a contractile phenotype to a synthetic phenotype (Fig 3C) and ameliorated stenosis and wall thickness of the MCA after SAH (Fig 3D). Using GW9662 repressed these effects.

The Inhibitory Mechanism of VSMC Phenotypic Transformation via PPARγ Partially Occurred Through the Suppression of FLAP/LTB_4 Expression

We constructed an adenoviral vector to knock down PPARγ in vivo to elucidate the molecular mechanisms of PPARγ-mediated VSMC phenotypic transformation. We designed two knocked down sequences of PPARγ to ensure high efficacy. Rats were grouped as follows: Sham, SAH+sh-con, SAH+sh-PPARγ1, SAH+sh-PPARγ2, SAH+MK886, and SAH+sh-PPARγ+MK886 (12 rats per group). Western blotting confirmed the effectiveness of shPPARγ1 and shPPARγ2 (Fig 4A), and immunofluorescence assays demonstrated that these shRNA decreased PPARγ expression in VSMCs (Fig 4B). Moreover, no statistically significant differences were observed between the SAH+sh-PPARγ1 and SAH+sh-PPARγ2 groups. Therefore, we chose shPPARγ2 in combination with MK886 (specific antagonist of FLAP) as the SAH+sh-PPARγ+MK886 group. Knockdown of PPARγ aggravated the phenotypic transformation of VSMCs from the contractile to the synthetic phenotype (Fig 4A), increased LTB_4 expression (Fig 4C) and exacerbated the deterioration of the neurological function (Fig 4D). However, the use of MK-886 partially reduced these effects. Therefore, we speculated that activation of PPARγ inhibited the expression of FLAP and LTB_4, resulting in the inhibition of the phenotypic transformation of VSMCs after SAH.

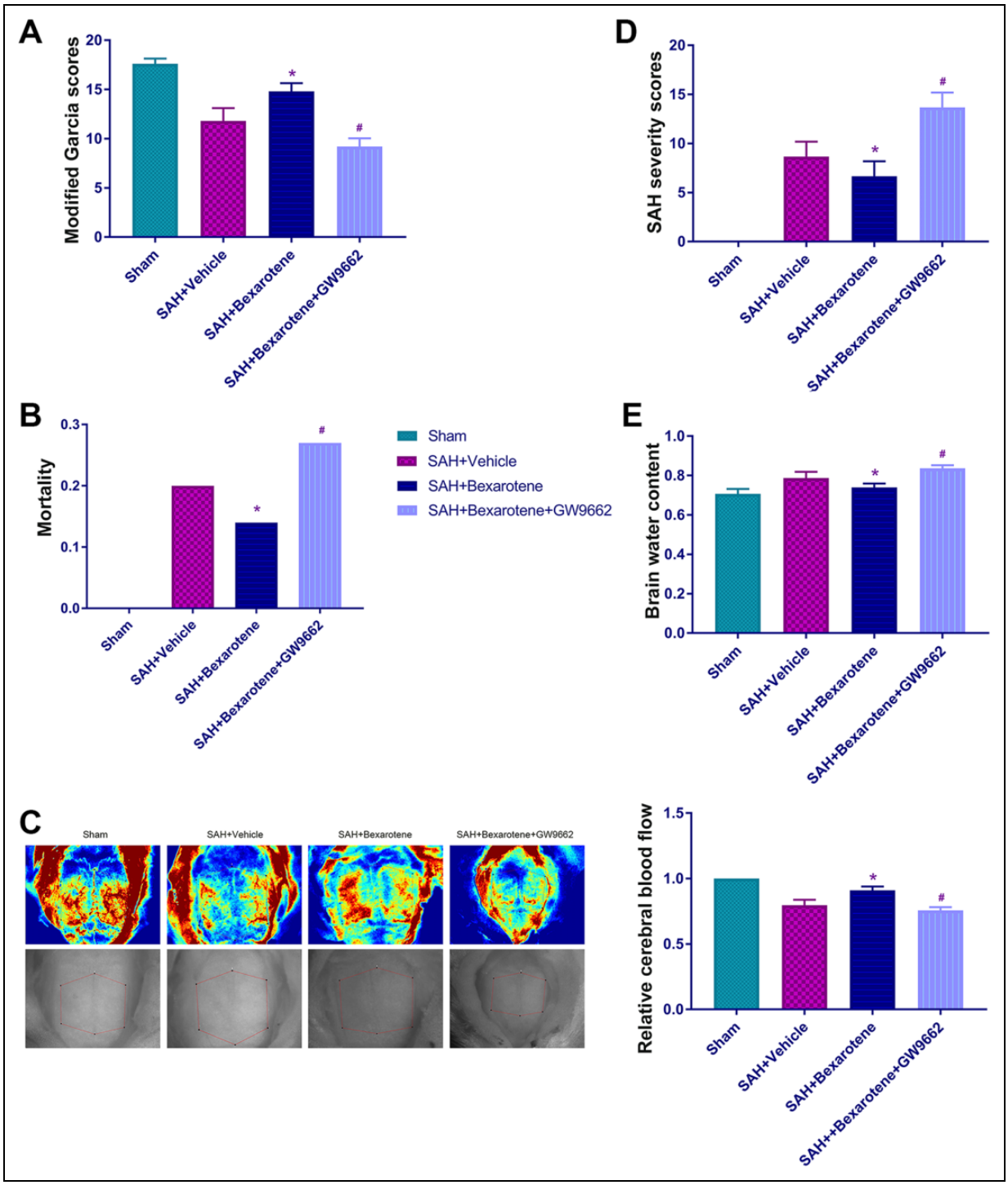

Figure 2. Bexarotene reduces neurological impairment and relieves ischemia after SAH via PPARγ activation. (A) Modified Garcia scores. (B) Mortality. (C) Representative images of cerebral cortical blood flow detected using laser speckle and quantitative analysis of cortical cerebral blood flow. (D) SAH severity scores. (E) Brain water content in Sham group, SAH+vehicle group, SAH+bexarotene group, and SAH+bexarotene+GW9662 group (*P<0.05 versus SAH+vehicle group, #P<0.05 versus SAH+bexarotene group; n=12, with 12 used for modified Garcia scoring and SAH severity scoring and cerebral blood flow measurements and 4 used for brain water content). The same rats were used in Fig 2 and Fig 3 and belonged to experimental part 2.
PPARγ: peroxisome proliferator-activated receptor gamma; SAH: subarachnoid hemorrhage.

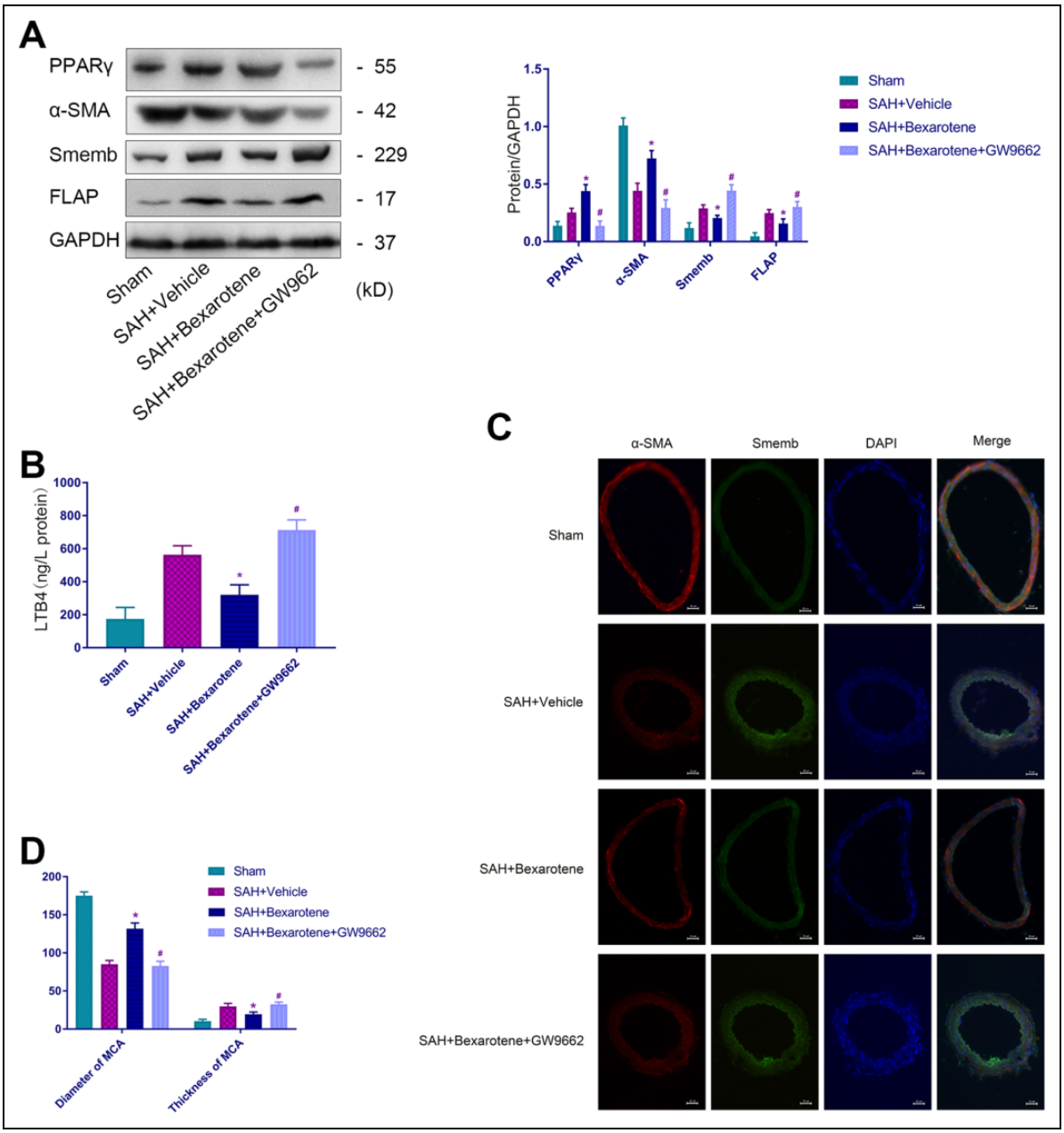

Figure 3. Bexarotene inhibits VSMC phenotypic transformation by activating PPARγ after SAH. (A) Representative immunoblots and representative quantitative analysis for α-SMA, Smemb, PPARγ and FLAP. (B) The expression of LTB_4. (C) Representative immunofluorescence staining for the middle cerebral artery of α-SMA (red), Smemb (green), and DAPI (blue; scale bar, 20 μm). (D) Quantitative analysis of the diameter and the thickness of the MCA in Sham group, SAH+vehicle group, SAH+bexarotene group, and SAH+bexarotene+GW9662 group (*P<0.05 versus SAH+vehicle group, #P<0.05 versus SAH+bexarotene group; n=12, with 4 used for western blotting and ELISA and 4 used for IF).
α-SMA: α-smooth muscle actin; DAPI: 4′,6-diamidino-2-phenylindole; ELISA: enzyme-linked immunosorbent assay; FLAP: 5-lipoxygenase-activating protein; IF, immunofluorescence; LTB_4: leukotriene B4; PPARγ: peroxisome proliferator-activated receptor gamma; SAH: subarachnoid hemorrhage; Smemb: embryonic smooth muscle myosin heavy chain.

Discussion

After SAH, a series of reactions were triggered, including altered vasoreactivity, microvascular constriction, increased endothelial inflammation and leukocyte-endothelial interactions, disruption of the blood–brain barrier, increased microthrombi and pathological inversion of neurovascular coupling[32]. These pathophysiological changes in the CNS interfere with the autoregulation of cerebral blood flow, which aggravates cerebral ischemia and hypoxia and causes neurological impairment[33,34]. Animal experiments have

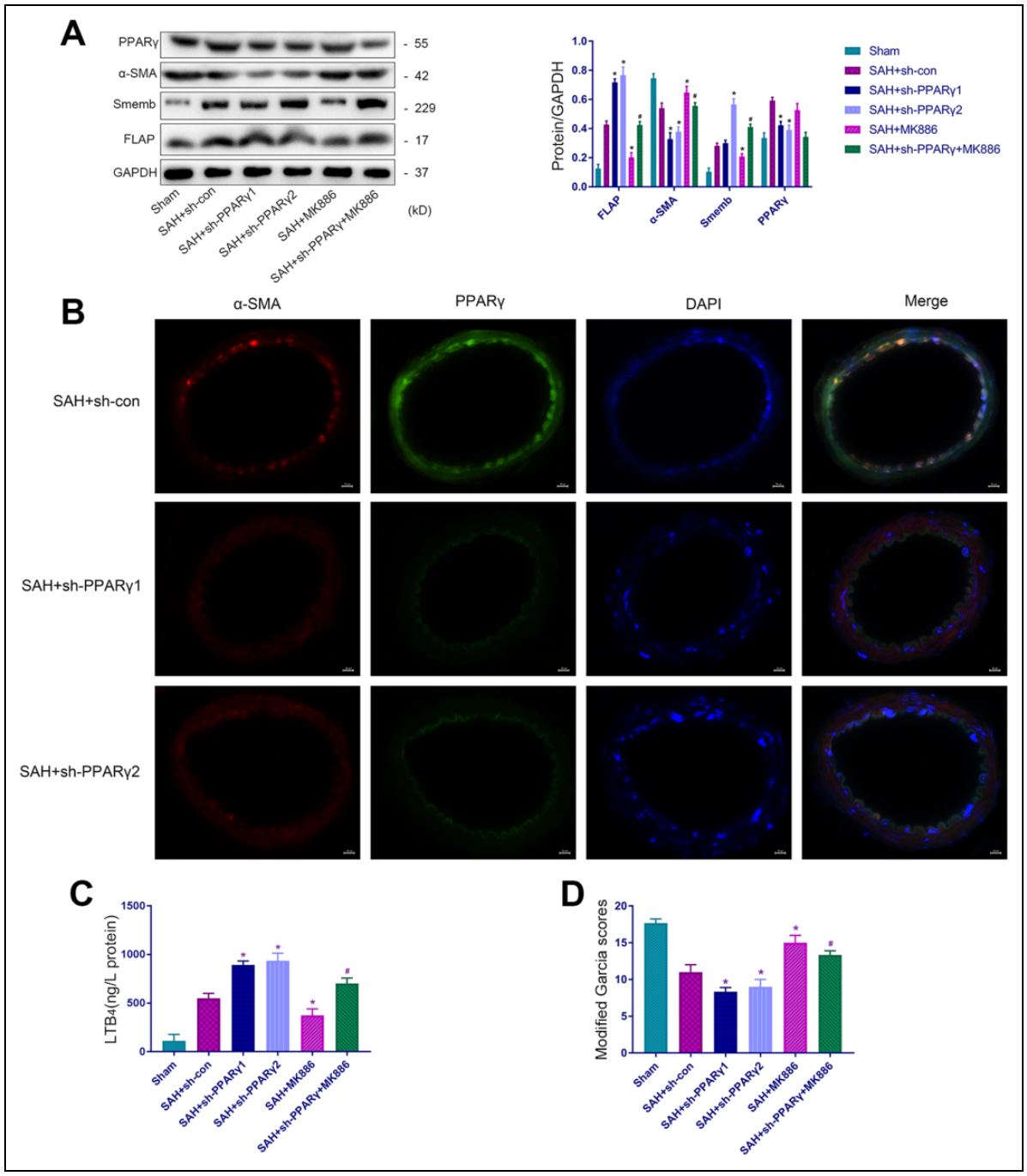

Figure 4. PPARγ activation inhibits the phenotypic transformation of VSMCs partially by suppressing FLAP/LTB_4 expression. (A) Representative immunoblots and representative quantitative analyses of α-SMA, Smemb, PPARγ and FLAP. (B) Representative IF staining of the middle cerebral artery for α-SMA (red), PPARγ (green), and DAPI (blue). Scale bar, 20 μm. (C) The expression of LTB_4. (D) Modified Garcia scores in Sham, SAH+sh-con, SAH+sh-PPARγ1, SAH+sh-PPARγ2, SAH+MK-886, and SAH+sh-PPARγ+MK-886 groups (*P<0.05 versus SAH+si-con group, #P<0.05 versus SAH+sh-PPARγ2 group). (D) (n=12, with 12 used for modified Garcia scores, 6 used for western blotting and ELISA and 6 used for IF).

α-SMA: α-smooth muscle actin; DAPI: 4′,6-diamidino-2-phenylindole; ELISA: enzyme-linked immunosorbent assay; FLAP: 5-lipoxygenase-activating protein; IF, immunofluorescence; LTB_4: leukotriene B4; PPARγ: peroxisome proliferator-activated receptor gamma; SAH: subarachnoid hemorrhage; Smemb: embryonic smooth muscle myosin heavy chain; VSMC: vascular smooth muscle cell.

demonstrated that calcium channel blockers reduce cerebral vasospasms[35]. The clinical use of calcium channel blockers, such as nimodipine and fasudil, also reduced the incidence of cerebral vasospasms and delayed cerebral ischemia; however, no significant improvement in patient outcomes was observed[36]. Therefore, other mechanisms may potentially

affect the perfusion of cerebral blood flow. VSMCs are known to play important roles in stabilizing vascular tone and regulating blood flow. The vascular system is damaged after stroke, and VSMCs protect our brain by promoting the rescue of ischemic penumbra and preserving the neurovascular unit. This process may be due to arterial smooth muscle cells with contractile phenotypes, which have the ability to regulate the balance of cerebral blood flows. VSMCs enhanced the vasodilatation and vasoconstriction abilities of arteries, which was accompanied by the recovery of cerebral blood flow and neurological function[32,37].

VSMCs in normal blood vessels adopt a contractile phenotype, wherein they primarily express proteins that regulate cell contraction, such as α-SMA and smooth muscle myosin heavy chains (SM-MHCs)[38]. However, VSMCs retain considerable plasticity and undergo phenotypic transformation from a contractile to a synthetic phenotype under pathological circumstances. VSMCs with a synthetic phenotype exhibit increased proliferation, migration and synthesis of extracellular matrix components, expressing specific protein markers, such as Smemb[39,40]. However, this phenotypic transformation contributes to the development or progression of vascular diseases, including atherosclerosis, asthma, and hypertension[41–43].The present study established SAH models using intravascular puncture. We found that VSMCs transformed from a contractile phenotype to a synthetic phenotype after SAH. The neurological deficits and cerebral cortical blood flow were also reduced. Therefore, we speculated that the pathophysiological process of VSMC phenotypic transformation may be involved in regulating neurovascular function after SAH. In this study, we performed an external carotid artery endovascular puncture in SD rats to establish SAH and found the phenotypic transformation of cerebral VSMCs. In addition, we found PPARγ and FLAP participated in the neurovascular injury process after SAH.

The United States Food and Drug Administration approved bexarotene some years ago for the clinical treatment of refractory cutaneous T-cell lymphoma[20]. However, bexarotene was not clinically indicated for SAH. Our group previously found that bexarotene relieved motor deficits and improved the spatial memory of rats after traumatic brain injury (TBI)[28,44]. Moreover, Cramer et al. found bexarotene improved the neurological function of rats with Alzheimer's disease[19]. Mechanistically, bexarotene activated retinoid X receptors (RXR), promoted RXR to form heterodimers with PPARγ, causing activation of PPARγ. PPARγ, also called NR1C3, is a ligand-modulated transcription factor belonging to the nuclear hormone receptor superfamily. PPARγ is a therapeutic target for treating type II diabetes[45]. Studies have shown that serine/threonine kinase (Bcr) activation inhibited the transcriptional activity of PPARγ, promoted VSMC inflammation and proliferation, leading to neointimal response after vascular injury[16]. In addition, Zhang et al. demonstrated that rosiglitazone inhibited VSMC transformation from contractile to synthetic phenotypes and prevented hypertension-related vascular disorders by activating PPARγ in hypertensive rats[17]. In addition, Yang et al. found that rosiglitazone inhibits VSMC phenotypic transformation by activating PPARγ/PKG and reduces neointimal hyperplasia after angioplasty[18]. The aforementioned studies suggested that PPARγ activation can inhibit the phenotypic transformation of VSMCs. Nevertheless, the effect of bexarotene on the PPARγ-mediated phenotypic transformation of VSMCs has not been reported. Therefore, the present study explored the neurovascular protection of bexarotene after SAH. Side effects have been reported with the use of bexarotene, such as reversible hyperlipidemia, pathological hepatomegaly and significant body weight reduction[20]. Our previous experiment demonstrated that bexarotene effectively entered the CNS when injected intraperitoneally at 5 mg/kg per day, with no obvious toxic or adverse effects[28].

The present study examined the potentially protective mechanisms of bexarotene after SAH. We found that the phenotypic transformation of VSMCs was obvious three days after SAH. Moreover, PPARγ and FLAP levels also reached a relatively high level at this time. Therefore, we selected this time point to perform further neurobehavioral examinations, cerebral cortical blood flow tests, immunofluorescence, western blotting, and ELISA assays, among others, to explore the protective mechanism of bexarotene. We found bexarotene ameliorated the neurological function deficits, improved cerebral cortical blood flow regulation and reduced the phenotypic transformation of VSMCs from a contractile phenotype to a synthetic phenotype. Bexarotene also reduced mortality, decreased the severity of SAH, reduced brain edema and ameliorated cerebral ischemia after SAH. The specific antagonist of PPARγ, GW9662, reduced these effects. To our knowledge, this study is the first to observe neurovascular protection by bexarotene after SAH.

The current study found that bexarotene activated PPARγ and inhibited the expression of FLAP and LTB_4 after SAH. We expected that FLAP and LTB_4 participate in the pathophysiological process of PPARγ-mediated phenotypic transformation of VSMCs. Therefore, we performed mechanistic experiments to investigate this hypothesis. We performed PPARγ knockdown combined with the use of MK886 in rats. We concluded that FLAP and LTB_4 were involved in PPARγ-mediated VSMC phenotypic transformation using western blotting, ELISA, and behavioral tests. Moreover, we also demonstrated that PPARγ inhibited the phenotypic transformation of VSMCs by inhibiting FLAP and LTB_4 after SAH.

Our study had some limitations. We did not perform experiments on the mechanisms of VSMC phenotypic transformation using bexarotene in vitro. Moreover, RXR may activate other proteins and transcription factors that we did not study in this research. In the future, we plan to address these limitations and further investigate the potential protective role of bexarotene after SAH.

SAH is a severe disease, and the current available therapies are unsatisfactory. The results of the present study

suggest that bexarotene is a good candidate for developing novel promising therapeutics. Future studies should focus on the profound mechanisms of bexarotene in regulating the pathological processes of cerebral vascular smooth muscle after SAH. FLAP/LTB_4 should also be investigated to develop effective therapies after SAH.

Conclusion

Bexarotene inhibits the phenotypic transformation of VSMCs and improves neurological function and cerebral cortical blood flow via PPARγ after SAH. Bexarotene achieves this effect by partially inhibiting FLAP/LTB_4-dependent phenotypic transformation of VSMCs. VSMC-related studies will provide novel perspectives for researching SAH and developing therapeutic strategies to treat SAH.

Acknowledgments

We express special gratitude to the Chongqing Key Laboratory of Ophthalmology and Laboratory Research Central, the First Affiliated Hospital of Chongqing Medical University, China, for providing the experimental platform.

Authors' Contributions

Zhaosi Zhang, Zongduo Guo and Xiaochuan Sun conceived and designed the research. Zhaosi Zhang conducted and performed the experiments, analyzed the data and wrote the manuscript. Guosheng Zhao, Liu Liu, Junchi He, Rami Darwazeh, Han Liu, Hong Chen and Chao Zhou participated in the conduction of the experiments and helped perform the literature review.

Zhaosi Zhang, Guosheng Zhao, Rami Darwazeh, Zongduo Guo and Xiaochuan Sun reviewed and edited the manuscript. All authors read and approved the manuscript.

Ethics Approval and Consent to Participate

This study was approved by our institutional review board. Animals were used with the approval of the Ethics Committee of the First Affiliated Hospital of Chongqing Medical University and the Institutional Animal Care and Use Committee of Chongqing Medical University, China.

Statement of Human and Animal Rights

The care of all animals complied with the guidance for the care and use of laboratory animals.

Statement of Informed Consent

There are no human subjects in this article and informed consent is not applicable.

Declaration of Conflicting Interests

The author(s) declared no potential conflicts of interest with respect to the research, authorship, and/or publication of this article.

Funding

The author(s) disclosed receipt of the following financial support for the research, authorship, and/or publication of this article: This research was supported by the National Natural Science Foundation of China (81671160, 81571159).

Supplemental Material

Supplemental material for this article is available online.

References

1. Fujii M, Yan J, Rolland WB, Soejima Y, Caner B, Zhang JH. Early brain injury, an evolving frontier in subarachnoid hemorrhage research. Transl Stroke Res. 2013;4(4):432–446.
2. Zhang JH, Badaut J, Tang J, Obenaus A, Hartman R, Pearce WJ. The vascular neural network–a new paradigm in stroke pathophysiology. Nat Rev Neurol. 2012;8(12):711–716.
3. Zhang H, Jiang L, Guo Z, Zhong J, Wu J, He J, Liu H, He Z, Wu H, Cheng C, Sun X. PPARβ/δ, a novel regulator for vascular smooth muscle cells phenotypic modulation and vascular remodeling after subarachnoid hemorrhage in rats. Sci Rep. 2017;7:45234.
4. Wan W, Ding Y, Xie Z, Li Q, Yan F, Budbazar E, Pearce WJ, Hartman R, Obenaus A, Zhang JH, Jiang Y, Tang J. PDGFR-β modulates vascular smooth muscle cell phenotype via IRF-9/SIRT-1/NF-κB pathway in subarachnoid hemorrhage rats. J Cereb Blood Flow Metab. 2018;0271678X18760954.
5. Willis AI, Pierre-Paul D, Sumpio BE, Gahtan V. Vascular smooth muscle cell migration: current research and clinical implications. Vasc Endovasc Surg. 2004;38(1):11–23.
6. Funk CD. Prostaglandins and leukotrienes: advances in eicosanoid biology. Science. 2001;294(5548):1871–1875.
7. Bäck M, Bu DX, Bränström R, Sheikine Y, Yan ZQ, Hansson GK. Leukotriene B4 signaling through NF-kappaB-dependent BLT1 receptors on vascular smooth muscle cells in atherosclerosis and intimal hyperplasia. Proc Natl Acad Sci U S A. 2005;102(48):17501–17506.
8. Evans JF, Ferguson AD, Mosley RT, Hutchinson JH. What's all the FLAP about?: 5-lipoxygenase-activating protein inhibitors for inflammatory diseases. Trends Pharmacol Sci. 2008;29(2):72–78.
9. Peters-Golden M, Brock TG. 5-Lipoxygenase and FLAP. Prostaglandins Leukot Essent Fatty Acids. 2003;69(2–3):99–109.
10. Yu Z, Ricciotti E, Miwa T, Liu S, Ihida-Stansbury K, Landesberg G, Jones PL, Scalia R, Song WC, Assoian RK, FitzGerald GA. Myeloid cell 5-lipoxygenase activating protein modulates the response to vascular injury. Circ Res. 2013;112(3):432–440.
11. Sobrado M, Pereira MP, Ballesteros I, Hurtado O, Fernández-López D, Pradillo JM, Caso JR, Vivancos J, Nombela F, Serena J, Lizasoain I, Moro MA. Synthesis of lipoxin A4 by 5-lipoxygenase mediates PPARgamma-dependent, neuroprotective effects of rosiglitazone in experimental stroke. J Neurosci. 2009;29(12):3875–3884.
12. Adrian TE, Hennig R, Friess H, Ding X. The role of PPARgamma receptors and leukotriene B(4) receptors in mediating the effects of LY293111 in pancreatic cancer. PPAR Res. 2008;2008:827096.
13. Ballesteros I, Cuartero MI, Pradillo JM, de la Parra J, Pérez-Ruiz A, Corbí A, Ricote M, Hamilton JA, Sobrado M, Vivancos J, Nombela F, Lizasoain I, Moro MA. Rosiglitazone-induced CD36 up-regulation resolves inflammation by

PPARgamma and 5-LO-dependent pathways. J Leukoc Biol. 2014;95(4):587–598.
14. Xie Z, Huang L, Enkhjargal B, Reis C, Wan W, Tang J, Cheng Y, Zhang JH. Recombinant Netrin-1 binding UNC5B receptor attenuates neuroinflammation and brain injury via PPARgamma/NFkappaB signaling pathway after subarachnoid hemorrhage in rats. Brain Behav Immun. 2017;69:190–202.
15. Gu C, Wang Y, Li J, Chen J, Yan F, Wu C, Chen G. Rosiglitazone attenuates early brain injury after experimental subarachnoid hemorrhage in rats. Brain Res. 2015;1624:199–207.
16. Alexis JD, Wang N, Che W, Lerner-Marmarosh N, Sahni A, Korshunov VA, Zou Y, Ding B, Yan C, Berk BC, Abe J. Bcr kinase activation by angiotensin II inhibits peroxisome-proliferator-activated receptor gamma transcriptional activity in vascular smooth muscle cells. Circ Res. 2009;104(1):69–78.
17. Zhang L, Xie P, Wang J, Yang Q, Fang C, Zhou S, Li J. Impaired peroxisome proliferator-activated receptor-gamma contributes to phenotypic modulation of vascular smooth muscle cells during hypertension. J Biol Chem. 2010;285(18):13666–13677.
18. Yang HM, Kim BK, Kim JY, Kwon YW, Jin S, Lee JE, Cho HJ, Lee HY, Kang HJ, Oh BH, Park YB, Kim HS. PPARgamma modulates vascular smooth muscle cell phenotype via a protein kinase G-dependent pathway and reduces neointimal hyperplasia after vascular injury. Exp Mol Med. 2013;45:e65.
19. Cramer PE, Cirrito JR, Wesson DW, Lee CY, Karlo JC, Zinn AE, Casali BT, Restivo JL, Goebel WD, James MJ, Brunden KR, Wilson DA, Landreth GE. ApoE-directed therapeutics rapidly clear beta-amyloid and reverse deficits in AD mouse models. Science. 2012;335(6075):1503–1506.
20. Duvic M, Hymes K, Heald P, Breneman D, Martin AG, Myskowski P, Crowley C, Yocum RC. Bexarotene is effective and safe for treatment of refractory advanced-stage cutaneous T-cell lymphoma: multinational phase II-III trial results. J Clin Oncol. 2001;19(9):2456–2471.
21. Riancho J, Berciano MT, Ruiz-Soto M, Berciano J, Landreth G, Lafarga M. Retinoids and motor neuron disease: potential role in amyotrophic lateral sclerosis. J Neurol Sci. 2016;360:115–120.
22. Bomben V, Holth J, Reed J, Cramer P, Landreth G, Noebels J. Bexarotene reduces network excitability in models of Alzheimer's disease and epilepsy. Neurobiol Aging. 2014;35(9):2091–2095.
23. McFarland K, Spalding TA, Hubbard D, Ma JN, Olsson R, Burstein ES. Low dose bexarotene treatment rescues dopamine neurons and restores behavioral function in models of Parkinson's disease. ACS Chem Neurosci. 2013;4(11):1430–1438.
24. Tunctan B, Kucukkavruk SP, Temiz-Resitoglu M, Guden DS, Sari AN, Sahan-Firat S. Bexarotene, a selective RXRalpha agonist, reverses hypotension associated with inflammation and tissue injury in a rat model of septic shock. Inflammation. 2018;41(1):337–355.
25. Cai W, Yang T, Liu H, Han L, Zhang K, Hu X, Zhang X, Yin KJ, Gao Y, Bennett MVL, Leak RK, Chen J. Peroxisome proliferator-activated receptor γ (PPARγ): a master gatekeeper in CNS injury and repair. Prog Neurobiol. 2018;163–164:27–58.
26. Culman J, Zhao Y, Gohlke P, Herdegen T. PPAR-gamma: therapeutic target for ischemic stroke. Trends Pharmacol Sci. 2007;28(5):244–249.
27. Muroi C, Fujioka M, Marcacher S, Fandino J, Keller E, Iwasaki K, Mishima K. Mouse model of subarachnoid hemorrhage: technical note on the filament perforation model. Acta Neurochir Suppl. 2015;120:315–20.
28. Zhong J, Cheng C, Liu H, Huang Z, Wu Y, Teng Z, He J, Zhang H, Wu J, Cao F, Jiang L, Sun X. Bexarotene protects against traumatic brain injury in mice partially through apolipoprotein E. Neuroscience. 2017;343:434–448.
29. Teng Z, Jiang L, Hu Q, He Y, Guo Z, Wu Y, Huang Z, Cao F, Cheng C, Sun X, Guo Z. Peroxisome proliferator-activated receptor β/δ alleviates early brain injury after subarachnoid hemorrhage in rats. Stroke. 2016;47(1):196–205.
30. Sugawara T, Ayer R, Jadhav V, Zhang JH. A new grading system evaluating bleeding scale in filament perforation subarachnoid hemorrhage rat model. J Neurosci Methods. 2008;167(2):327–334.
31. Miller D, Forrester K, Leonard C, Salo P, Bray RC. ACL deficiency impairs the vasoconstrictive efficacy of neuropeptide Y and phenylephrine in articular tissues: A laser speckle perfusion imaging study. J Appl Physiol. 2005;98(1):329–333.
32. Tso MK, Macdonald RL. Subarachnoid hemorrhage: a review of experimental studies on the microcirculation and the neurovascular unit. Transl Stroke Res. 2014;5(2):174–189.
33. Ohkuma H, Suzuki S, Ogane K. Phenotypic modulation of smooth muscle cells and vascular remodeling in intraparenchymal small cerebral arteries after canine experimental subarachnoid hemorrhage. Neurosci Lett. 2003;344(3):193–196.
34. Maddahi A, Povlsen GK, Edvinsson L. Regulation of enhanced cerebrovascular expression of proinflammatory mediators in experimental subarachnoid hemorrhage via the mitogen-activated protein kinase kinase/extracellular signal-regulated kinase pathway. J Neuroinflamm. 2012;9:274–289.
35. Marbacher S, Neuschmelting V, Graupner T, Jakob SM, Fandino J. Prevention of delayed cerebral vasospasm by continuous intrathecal infusion of glyceroltrinitrate and nimodipine in the rabbit model in vivo. Intensive Care Med. 2008;34(5):932–938.
36. Vergouwen MD. Vasospasm versus delayed cerebral ischemia as an outcome event in clinical trials and observational studies. Neurocrit Care. 2011;15(2):308–311.
37. Lo EH, Broderick JP, Moskowitz MA. t-PA and proteolysis in the neurovascular unit. Stroke. 2004;35(2):354–356.
38. Alexander MR, Owens GK. Epigenetic control of smooth muscle cell differentiation and phenotypic switching in vascular development and disease. Annu Rev Physiol. 2012;74:13–40.
39. Owens GK. Molecular control of vascular smooth muscle cell differentiation and phenotypic plasticity. Novartis Found Symp. 2007;283:174–191.

40. Somlyo AP, Somlyo AV. $Ca2^{+}$ sensitivity of smooth muscle and nonmuscle myosin II: Modulated by G proteins, kinases, and myosin phosphatase. Physiol Rev. 2003;83(4): 1325–1358.
41. Yoshida T, Owens GK. Molecular determinants of vascular smooth muscle cell diversity. Circ Res. 2005;96(3):280–291.
42. Hao H, Gabbiani G, Bochaton-Piallat ML. Arterial smooth muscle cell heterogeneity: Implications for atherosclerosis and restenosis development. Arterioscler Thromb Vasc Biol. 2003; 23(9):1510–1520.
43. Davis-Dusenbery BN, Wu C, Hata A. Micromanaging vascular smooth muscle cell differentiation and phenotypic modulation. Arterioscler Thromb Vasc Biol. 2011;31(11):2370–2377.
44. Zhong J, Jiang L, Huang Z, Zhang H, Cheng C, Liu H, He J, Wu J, Darwazeh R, Wu Y, Sun X. The long non-coding RNA Neat1 is an important mediator of the therapeutic effect of bexarotene on traumatic brain injury in mice. Brain Behav Immun. 2017;65:183–194.
45. Berger J, Moller DE. The mechanisms of action of PPARs. Annu Rev Med. 2002;53:409–435.